On the Fate of Little Red Dots

Andrés Escala[1], Lucas Zimmermann[2], Sebastián Valdebenito[1], Marcelo C. Vergara[3], Dominik R.G. Schleicher[4], Matías Liempi[4]

1 Departamento de Astronomía, Universidad de Chile, Casilla 36-D, Santiago, Chile.

2 Department of Astronomy, Yale University, New Haven, CT 06511, USA

3 Astronomisches Rechen-Institut, Zentrum fur Astronomie, University of Heidelberg, Monchhofstrasse 12-14, 69120, Heidelberg, Germany

4 Dipartimento di Fisica, Sapienza Università di Roma, Piazzale Aldo Moro 5, 00185 Rome, Italy

Correspondence to: aescala@das.uchile.cl

ABSTRACT

We study the stability and possible fates of Little Red Dots, under the stellar-only interpretation of their observational features. This is performed by a combination of analyzing the relevant timescales in their stellar dynamics and also, the application of recent numerical results on the evolution of the densest stellar systems. We study different scenarios for the evolution of Little Red Dots and conclude that in a fair fraction of those systems, the formation of a massive black hole by runaway collisions seems unavoidable, in all the possibilities studied within the stellar-only interpretation. We conclude that Little Red Dots are the most favourable known places to find a recently formed massive black hole seed, or in the process of formation, most probably formed directly in the supermassive range.

Subject headings: galaxies: galactic nuclei- black hole: formation

1. Introduction

The *James Webb* Space Telescope (JWST) revolutionized our vision of the early universe, detecting $z > 14$ galaxies (e.g., R. Naidu et al. 2025), and uncovering a new population of high-redshift sources that had eluded earlier telescopes: the Little Red Dots (LRDs; D.

D. Kocevski et al. 2023; Y. Harikane et al. 2023; J. Matthee et al. 2024), which are characterized to be extremely compact and red. More striking, detections of LRDs concentrate only in the redshift range $4 < z < 8$ (D. D. Kocevski et al. 2025), making this population of galaxies observable during a cosmic period of only $\lesssim 1$ Gyr, i.e. less than one orbital period for a Milky Way-type galaxy (comparable in stellar mass to the most massive LRDs), thus appearing as almost transitory objects even for galactic timescales and certainly, for cosmological ones.

Two main interpretations has been suggested for LRDs, each peculiar and not previously observed before JWST. The first one, that LRDs host a super-Massive Black Hole (MBH) at their centers due to the presence of broad Balmer emission lines (R. Maiolino et al. 2024; J. E. Greene et al. 2024). However, most LRDs are undetected in X-rays, even in deep stacking analyses (T. T. Ananna et al. 2024; F. Pacucci & R. Narayan 2024; P. Madau & F. Haardt 2024; R. Maiolino et al. 2025). Assuming that the black holes still are present, they seem to be over-massive respect to their host (F. Pacucci et al. 2023; K. Inayoshi & K. Ichikawa 2024; E. Durodola et al. 2025), compared to the masses expected from extrapolating the local relations (J. Magorrian et al. 1998, L. Ferrarese & D. Merritt 2000; K. Gebhardt et al. 2000).

The second interpretation is that they are intensely star-forming dusty galaxies (Akins et al 2024), but the cores reach extreme stellar densities being the densest stellar systems ever observed (Guia et al. 2024). The latter comes from their compactness, one of the most striking features of the LRDs, with typical effective radii $\sim$100 pc are (on average) an order of magnitude more compact than the smallest galaxies previously observed. Moreover, the widths of the Balmer broad lines can also be explained by the stellar velocity dispersion at the cores of these system (A. Loeb 2024; J. F. W. Baggen et al. 2024), generating velocities of $\sim$1500 km s^{-1}, around factor 4 larger than the maximum velocity dispersion documented in the nearby Universe ($\sigma = 444\,\mathrm{kms}^{-1}$; Salviander et al 2008), whose long term stability is probably not viable (A. Escala 2025).

The goal of this paper is to show that regardless of the interpretation, the expected fate of LRDs is that will eventually host a MBH (or become one in the most extreme cases). This is because (even) under the stellar only interpretation, LRDs extreme stellar densities implies that a fair fraction (up-to unity) of their inner regions will unavoidably end in a MBH, expected also to be over-massive with respect to the host. This is based in the scenario outlined in A. Escala (2021), in which MBHs are formed in-situ at galactic nuclei as (partially or totally) failed stellar systems. This paper is organized as follows, we start studying the stability of LRDs under the stellar-only interpretation in §2, analyzing the relevant timescales for stability in §2.1 and possible unstable outcomes in §2.2. In §3, we

will discuss a summary of the results and conclusions achieved.

2. Stability of LRDs in the Stellar-Only Interpretation

In this section we will study the long term stability of LRDs, in the context of an scenario for MBH seeds that forms by direct collapse in galactic nuclei from a failed stellar system, that is unstable due to runaway stellar collisions. This was proposed in Escala (2021), that studied the stability of stellar systems in galactic nuclei and compared with the observed properties of galactic nuclei (MBHs and Nuclear Stellar Clusters; NSCs), being able to explain the relative trends observed in the masses, efficiencies, and scaling relations between MBHs and NSCs. Several numerical results has latter supported the viability of this scenario, focused on different aspects of it (M.C. Vergara et al 2023, 2024, 2025a,b), including the first state-of-art (and one particle per star) N-body simulation able to form a Very Massive Star (VMS; which subsequently collapses to a MBH seed) that reaches the $\sim 10^5\,M_\odot$ mass scale (M.C. Vergara et al 2025a) from runaway stellar collisions, within the DRAGON suite of simulations (L. Wang et al 2016, M. Arca-Sedda et al 2024).

2.1. Relevant Timescales in the Stability of Stellar Systems

There are two distinct regimes when the stellar system in galactic nuclei may become globally unstable, being determined by relative values of the relaxation t_{relax} and collision t_{coll} timescales (Escala 2021): $t_{relax} < t_{coll}$ and $t_{coll} < t_{relax}$, when these (average) timescales are dynamically relevant (i.e. comparable or shorter than the age of the system t_{age}). Stellar systems with $t_{relax} < t_{coll}$ ($< t_{age}$) are initially globally unstable, but are able to readjust before collisions are triggered overall in the system, since the cluster will expand before (on few relaxation times t_{relax}; Henon 1965; Gieles et al. 2012), due to two-body encounters which guarantees the global stability of the stellar system. However, on the same timescale the core will undergo collapse (Cohn 1980; Portegies Zwart & McMillan 2002) enhancing the runaway collisions within the core. These runaway collisions are expected to lead the formation of a BH within the core and the predicted final state is the coexistence of a MBH and a NSC (Escala 2021).

This first regime, $t_{relax} < t_{coll}$ ($< t_{age}$), has been recently tested numerically by means of direct N-body simulations (M.C. Vergara et al 2023, 2024, 2025a,b), in particular, being able to show that the efficiency in the formation of the MBH by runaway stellar collisions exponentially increases (before saturation towards 1), with MBH efficiencies up to 50% of

the final cluster mass, for systems with average collision timescales t_{coll} that are comparable to the age of the system t_{age} (M.C. Vergara et al 2023). This result was also shown to be valid (M.C. Vergara et al 2024) for diversity of stellar systems (NSCs, globular cluster (GCs), and ultra-compact dwarf galaxies (UCDs)) and methods (both numerical simulations and observations fullfil it, encompassing various initial conditions, initial mass functions, and evolutionary scenarios). In principle, with MBH efficiencies $\sim 10{-}50\%$ a $10^{6-7}M_{\odot}$ stellar cluster could form a MBH seed directly in the super-massive regime, compared to alternative mechanisms that are also based on runaway stellar collisions and the collapse of a VMS, but predicts MBHs seeds in the intermediate-mass regime (i.e. A. Askar et al 2021, E. González-Prieto et al 2024, A. Rantala et al. 2025).

In the another regime when $t_{coll} < t_{relax}$ ($< t_{age}$), the stellar system will not able to adjust before collisions are triggered everywhere, which are highly inelastic and efficiently converts the orbital motions that supports the cluster (against its self-gravity) into heat (that subsequently can be radiated away), leading to a possible collapse of the system as a whole on to a MBH. Under this regime, no stellar system should survive in the long term and for that reason, we will subsequently call it 'Forbidden Stellar Zone', particularly to the region of cluster parameters (i.e. mass and radius), where no stellar system is expected to survive. Unfortunately, simulations in this regime are extremely expensive numerically, so restrictive that no direct N-body simulations has been performed yet for systems under this regime, but simulations M.C. Vergara et al (2023, 2024, 2025a,b) are suggestive since even in the $t_{relax} < t_{coll}$ regime, an exponential increase is found that reaches BH efficiencies upto 50% of the final (MBH + stellar) system.

One of the advantages of the simple picture outlined in Escala (2021), is that it is possible to evaluate the previously mentioned regimes for observed systems with measured and radius R and masses M, since the relevant timescales can be expressed in just those two quantities, under few assumptions such as being virialized systems (i.e. with a velocity dispersion $\sigma = \sqrt{GM/R}$). The collision timescale for virialized systems can be expressed as $t_{coll} = \sqrt{\frac{R}{GM(n\Sigma_0)^2}}$, where R and M are the radius and the mass of the system, G is the gravitational constant, Σ_0 is the effective cross-section and n is the number density of stars ($= \eta M/M_* R^3$, with $\eta = 3/4\pi$ for a uniform spherical system). The effective cross section Σ_0, counting the gravitational focusing is $\Sigma_0 = 16\sqrt{\pi}R_*^2(1+\Theta)$, where $\Theta = 9.54(\frac{M_* R_\odot}{M_\odot R_*})(\frac{100\,\mathrm{kms}^{-1}}{\sigma})^2$ is the Safronov number, with M_* and R_* being the typical masses and radius of the stars, respectively, and σ is the (rms) stellar velocity dispersion, which again can be expressed in terms of M and R as $\sigma = \sqrt{GM/R}$ using the virial theorem. Therefore, t_{coll} can be expressed only in terms of M and R for a system composed of stars with typical masses M_* and radius R_*. Same case for the relaxation time $t_{relax} = \frac{0.1N}{\ln N} t_{cross}$, where N is the total number of stars, which is simply $N = M/M_*$ if the system is composed of equal-mass stars,

and $t_{cross} = \sqrt{R^3/GM}$ is the crossing time for a virialized system, thus t_{relax} can also be expressed only in terms of M and R, for a system composed of stars with typical masses M_*.

Figure 1 shows both the collision and relaxation timescales, in a mass-radius plane compared to the current age of the Universe (i.e. $t_{age} = t_{H0} = 1.4 \times 10^{10}$yr, the maximum relevant time as an upper limit for the real ages) and for a stellar system (mainly) composed of solar mass stars. The solid black line displays the condition $t_{coll} = t_{H0}$, therefore, systems on the left side of the solid black line fulfill the condition $t_{coll} < t_{H0}$, thus collisions may be triggered everywhere in the system, contrarily to systems on the right side of the black line ($t_{coll} > t_{H0}$), where collisions should not be dynamically relevant (outside the core, if this collapses) and the system can be long term stable. Similar case for the dashed black one, that denotes the condition $t_{relax} = t_{H0}$, dividing the regions $t_{relax} < t_{H0}$ (left side to the dashed line) and $t_{relax} > t_{H0}$ (right side). The orange points displays the total masses and effective radius in NSC (Georgiev et al 2016). Black points denotes resolved MBHs and the white ones, unresolved MBHs (Gultekin et al. 2009). Black dotted line (upper left) denotes Scwardshild radius for a given mass, where real sizes of black holes should be, like the Event Horizon Telescope (2019) detection for M87 (black star just below the dotted line).

The solid black line in Figure 1 ($t_{coll} = t_{H0}$), clearly separates the population of resolved MBHs (black points) with the NSCs (orange) and unresolved MBHs (white ones, with properties diluted to the ones of the background stellar system and thus representative of it instead of the MBH; Escala 2021). The simplest interpretation is that stellar systems born on the left side of the solid black line, do not survive since it become globally unstable to runaway collisions and collapse to a MBH, in agreement with resolved MBHs (black points) being in that region of Figure 1 and contrarily, survived stellar systems born on the right side of the solid black line, in agreement with the location of orange and white points (NSCs and background stellar system of unresolved MBHs) in Figure 1. However, the discussed points are mainly below the intersection of solid and dashed lines, thus eventhough systems that born with $t_{coll} < t_{H0}$ are initially globally unstable, they have even shorter relaxation times ($t_{relax} < t_{coll}$) and the stellar system will be able to expand and survive before collapsing as a whole onto a MBH. Only their cores may become unstable and lead to the formation of a BH by runaway collisions within the core, being the predicted final state for those systems the possible coexistence of a MBH and a NSC (Escala 2021).

This simple picture was further supported recently by several direct N-body numerical calculations. M.C. Vergara et al (2023) showed that the efficiency in the formation of the MBH by runaway stellar collisions exponentially increases as t_{coll} becomes comparable to t_{age}, independent of having (even) shorter relaxation times, mainly because relaxation processes produces core collapse (and envelope expansion) but the efficiency is controlled by the

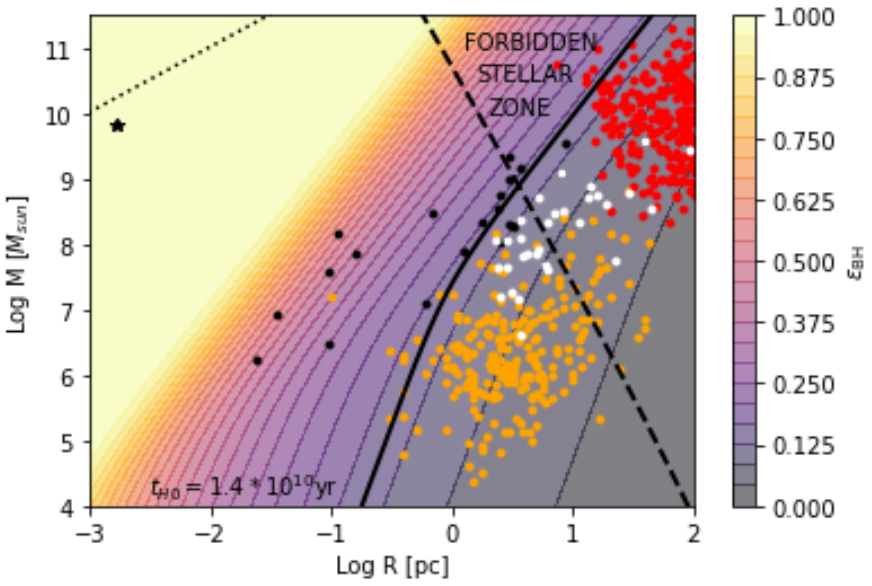

Fig. 1.— Total masses M and sizes R in color points for the following systems: resolved MBHs (black), unresolved MBHs (white), NSCs (orange) and LRDs (red). The solid black curve follows the condition $t_{coll}(M, R) = t_{H0}$ for a system of a given mass M and radius R (at the current age of the universe $t_{H0} = 1.4 \times 10^{10}$ yrs) and the dashed one, the condition $t_{relax}(M, R) = t_{H0}$. The color diagram denotes the black hole efficiency expected from $\epsilon_{BH} = (1 + \exp[-4.63(\log(M/M_{crit}) - 4)])^{-0.1}$ (M.C. Vergara et al 2023, 2024, 2025b), with M_{crit} coming from the condition $t_{coll}(M_{crit}) = t_{H0}$. Those efficiencies matches the expectations for the MBH formation scenario outlined in Escala (2021), where MBHs are formed from (partially/totally) failed stellar systems, by approaching towards 1 for resolved MBHs (black points) and being NSCs mainly in the range between 0.05 and 0.15 (coexistence of a MBH and a NSC; Escala 2021). The region called 'Forbidden Stellar Zone' fulfill the instability defined by $t_{coll} < t_{H0} (< t_{relax})$, where no stellar system is expected to survive, being most LRDs at the boundary of such instability (considering their upper limits in total effective radius).

collision time. M.C. Vergara et al (2024) expanded this finding to different stellar systems, including not only NSCs, but also GCs and UCDs, covering different initial conditions, stellar initial mass functions, and evolutionary paths, which can be fitted with an asymmetric sigmoidal curve, given by $\epsilon_{BH} = (1 + \exp[-4.63(\log(M/M_{crit}) - 4)])^{-0.1}$ (M.C. Vergara et al 2025b), where M_{crit} is the critical mass for a system with collision time comparable to the age of the system (i.e. $t_{coll}(M_{crit}) = t_{H0}$, for the purposes of this analysis). Figure 1 also displays such black hole formation efficiency ϵ_{BH} in the (background) color gradient, being

NSCs mainly in the range between 0.05 and 0.15, approaching towards 1 for resolved MBHs (i.e. if they were stellar clusters, should rapidly collapse to a MBH driven by runaway stellar collisions), in an overall agreement with their observed properties and also, supporting the scenario outlined in Escala (2021), where MBHs are formed from (partially/totally) failed stellar systems.

The position of LRDs in Figure 1, denoted by the red points (data taken from Akins et al 2024), is different from any other stellar system previously observed at lower z, since LRDs appear at the boundary of the region we called 'Forbidden Stellar Zone', located above the intersection of solid and dashed black lines, in the left side of the solid black line where no stellar system is expected to survive. Such region fulfill the instability defined by $t_{coll} < t_{H0}$, left side of the solid black line like the densest NSCs borned, but with a quantitative difference: in the mass range of LRDs (masses $\gtrsim 10^9 M_\odot$), the condition $\mathrm{t_{coll}} < \mathrm{t_{relax}}$ it is typically fulfilled furthermore. Therefore, LDRs with $t_{coll} < t_{H0}$ are on a different regime from unstable NSCs, without being able to expand due to relaxation processes, since $t_{H0} < t_{relax}$ for LRDs, thus candidates to be in the unexplored regime of collapsing as a whole due to the loss of orbital support by runaway stellar collisions. In the next section we will study possible outcomes for LRDs.

2.2. Globally Unstable Outcomes

In this section we will study the stability and possible fates for LRDs, exploring three possible avenues for such extremely dense stellar systems, with the aim of studying the viability for MBH formation triggered by runaway stellar collisions, under the stellar-only interpretation for LRDs observational features.

We will start computing the MBHs masses expected for LRDs from the numerical results of M.C. Vergara et al (2023, 2024, 2025a, b), although they are not strictly applicable to these systems. This is because for most LDRs $t_{coll} < t_{relax}$ (i.e. located above the intersection of dashed and solid lines in Fig 1), aversely to the numerical results of M.C. Vergara et al (2023, 2024, 2025a, b) that are strictly valid only in the regime $t_{relax} < t_{coll}$ and also, can only considered upper limits for BH masses expected in such regime since primordial binaries are not included in those numerical studies. This fact has quantitative differences, since when $t_{coll} < t_{relax}$, the system will not able to adjust (due to two-body relaxation) before collisions are triggered everywhere, leading to a possible collapse of the system as a whole on to a MBH (if in addition, $t_{coll} < t_{H0}$ is fulfilled, which is not the case for most LRDs if the measured upper limits in radius corresponds to their real sizes). On the other hand, no core collapse is expected for LRDs, since $t_{H0} < t_{relax}$ for theses systems and therefore, the initial growth of

the MBH should slow down. Therefore, to apply M.C. Vergara et al (2023, 2024, 2025a, b) results to LRDs, it is implicitly assumed that both processes compensates. This assumption could also be supported by the no dependence yet reported of the BH formation efficiency ϵ_{BH} on t_{relax} (i.e. negligible or secondary compared to the dependence on t_{coll} found in M.C. Vergara et al 2023, 2024).

Red points in Fig 2a shows the LRDs in a mass radius diagram. The solid black line displays again the condition $t_{coll} = t_{H0}$ and the dashed one, denotes the condition $t_{relax} = t_{H0}$, both computed at the age of the Universe $t_{H0} = 0.6 \times 10^9$yr, which corresponds to the time of appearance of LRDs in the universe (z $\sim$ 8). The position of LRDs avoids the forbidden stellar zone, with only one exception, besides all LRDs fulfilled the condition $t_{coll} < t_{relax}$ (i.e. masses larger than the intersection of the solid and dashed black curves). Figure 2a also displays the predicted black hole masses, in a contour plot with color gradient in the background, using the formation efficiency ϵ_{BH} computed numerically in M.C. Vergara et al (2025b), namely $M_{BH} = \epsilon_{BH} \times M = M \times (1 + \exp[-4.63\,(\log(M/M_{crit}) - 4)])^{-0.1}$. The bulk of the predicted masses for MBHs from the ϵ_{BH} in M.C. Vergara et al (2025b), are in the range between $\sim 5 \times 10^6 M_\odot$ and $\sim 10^{10} M_\odot$, incidentally in the same range observed for MBHs in the local universe.

In addition to the fact that M.C. Vergara et al (2023, 2024, 2025a, b) results are not strictly applicable to LRDs, there are two additional reasons for exploring a different interpretation for the evolution and possible fates of LRDs. The first one, is their transitory nature on a cosmological context, since this population observed during a cosmic period of only a Gyr in total (i.e. the timespan between z $\sim$ 4 and 8), possibly having individual lifespan of $\sim 10^8$ yrs (or less). The second one, is a direct consequence of their compactness: besides LRDs have typical effective radii $\sim$100 pc, in most cases these are only upper limits, possibly entering to the 'Forbidden Stellar Zone' if their real effective radii are considerable smaller than the measured upper limits. In Fig 2b, we start exploring the consequences of a lower effective radii than the measured upper limits and for that, we computed the conditions of $t_{coll} = t_{H0}$ (solid black lines) and $t_{relax} = t_{H0}$ (dashed black lines), at the cosmic age of appearance ($t_{H0} = 0.6 \times 10^9$yr or z $\sim$ 8) and disappearance ($t_{H0} = 1.5 \times 10^9$yr or z $\sim$ 4) of LRDs in the universe (D. D. Kocevski et al. 2024). The dotted line corresponds to the locus of the condition $t_{coll} = t_{relax}$ (for solar mass stars) at different cosmic times t_{H0}, which can be computed analytically and equivalent to the condition $\mathrm{R/R_\star} = \sqrt{\frac{1.2(1+\Theta)}{\sqrt{\pi}\mathrm{lnN}}}\,\mathrm{N}$, being $\mathrm{N}{=}M/M_\star$ and noting that $\Theta \approx 0.5$ when t_{coll} approaches t_{relax} (Escala 2025), leads to the simpler formula $\mathrm{R/R_\star} \approx \frac{1}{\sqrt{\mathrm{lnN}}}\,\mathrm{M/M_\star}$ valid for $t_{coll} = t_{relax}$. We see that this dotted line passes thru both intersections (between solid and dashed lines) on Fig 2b, as expected.

Fig 2b shows in red points the positions of LRDs for their upper limit sizes (i.e. same as

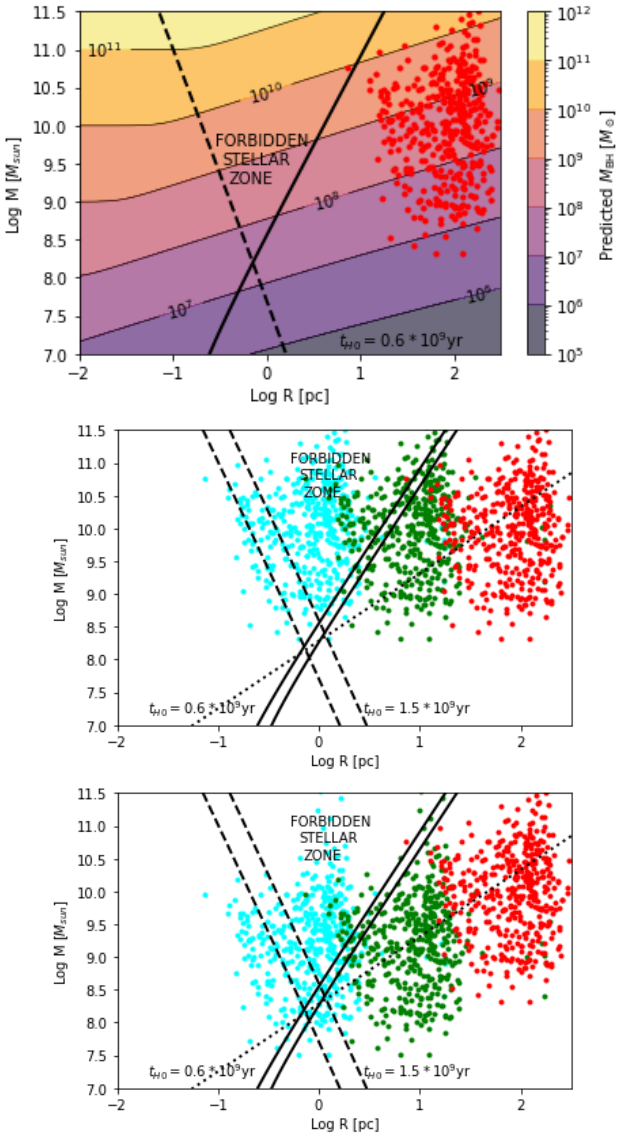

Fig. 2.— (a) Total masses M and radius R in red points for LRDs, the solid black curve following the condition $t_{coll}(M, R) = t_{H0}$ for the age of the universe at z∼8 ($t_{H0} = 0.6 \times 10^9$ yrs) and the dashed one, the condition $t_{relax}(M, R) = t_{H0}$. The color diagram denotes the predicted black hole mass M_{BH} expected from $M \times (1 + \exp[-4.63\,(\log(M/M_{crit}) - 4)])^{-0.1}$ (Vergara et al 2023, 2024, 2025b), predicting M_{BH} an approximate range between $5 \times 10^6 M_\odot$ and $10^{10} M_\odot$. (b) The positions of LRDs for the measured upper limit radius in red, in green LRDs positions assuming that their real effective radii corresponds to the 10% of the upper limits and in cyan, assuming that corresponds to the 1% of the upper limits in radius. The solid and dashed black curves denotes the same condition as in (a), but at the cosmic age of appearance ($t_{H0} = 0.6 \times 10^9$yr) and disappearance ($t_{H0} = 1.5 \times 10^9$yr) of LRDs. In the case of the green points, a fraction enters to the 'Forbidden Stellar Zone' ($t_{coll} < t_{H0} < t_{relax}$), while the cyan points it is more extreme, with most LRDs are in such situation. (c) Same as (b), now assuming that it is the core radius of the LRDs the one equals to the 10% (green) or 1% (cyan) of their measured effective radii, with most of the cores entering to the 'Forbidden Stellar Zone' for the case where LRDs core radius equals to the 1% of their measured radii.

in Figs 1 and 2a), in green LRDs positions assuming that their real effective radii corresponds to the 10% of the upper limits and in cyan, assuming that their real effective radii corresponds to the 1% of the measured upper limits. In the case of the green points (10% of the measured upper limits), a fraction enters to the 'Forbidden Stellar Zone' ($t_{coll} < t_{H0} < t_{relax}$), where it is expected that most of its mass end-up forming a massive black hole, with a minor fraction of stars possibly escaping from the system (i.e. becoming unbound in the formation process). The case of the cyan points (1% of the measured upper limits) it is clearly more extreme, with most LRDs are in such situation of ending as a whole forming a MBH. In the latter case, a big population of MBHs of $\gtrsim 10^{10} M_{\odot}$ it is predicted, which is currently unobserved in the Universe, suggesting that the real radii should not be typically much less than 10% of the observed upper limits, or that LRDs masses are considerably overestimated.

A third (and less extreme) possibility it is explored in Fig 2c, assuming that it is the core radius of the LRDs the one equals to the 10% (or 1%) of their measured (total) effective radii. Assuming a Plummer profile for the LRDs, the core radius can be defined where the projected mass density drops to half its central value, which corresponds to $r_c = a\sqrt{\sqrt{2}-1} \approx 0.64a$ (Dejonghe 1987, being a the Plummer radius), with an enclosed core mass $M(< r_c) = M_{tot} r_c^3/(r_c^2 + a^2)^{3/2}$ being equal to 15.7% of their total masses M_{tot}. Fig 2c shows in green points LRDs cores with radius equals to the 10% of their measured effective radii and the cyan ones, equals to the 1% of their effective radii. For this case, from a fraction of LRDs cores enters to the 'Forbidden Stellar Zone' (10% core radius case), to most of them for the case where LRDs cores have radius equals to the 1% of their measured effective radii (in both cases it is assumed a core mass being equal to 15.7% of their total masses). Therefore, under this scenario the LRDs should be forming MBHs mostly in the range of $\sim 3\times10^7 - 3\times10^{10}\, M_{\odot}$ (if all the core ends up collapsing onto a MBHs, with lower masses if a fraction of stars scapes from the core in the process). It is important to note, that this 'core collapse' (onto a MBH) differs from the standard one studied in stellar systems, since it is not driven by 2-body relaxation (because $t_{relax} > t_{H0}$) and instead, directly by runaway stellar collisions. The quantitative difference with the 2-body relaxation standard 'core collapse', will be that this 'core collapse' happens without an expansion of the envelope.

In summary, in the three different possibilities analyzed, the formation of a MBH seems unavoidable, for all the discussed possible scenarios under the stellar-only interpretation for LRDs. This is mainly due to the extreme stellar densities in LRDs inferred from JWST's observations, being almost unavoidable the onset of violent stellar collision that triggers a global instability of their cores (at the very least), probably forming MBHs directly in the supermassive range. Another recent work, F. Pacucci et al 2025, also predicts the formation of BHs in LRDs but in a considerably lower mass range (10^{3-4}M$_{\odot}$), using a variety of approaches that, however, do not include the role of the collision timescale in their analysis.

These approaches ranges from more appealing ones like N-body calculations of dense stellar systems (for a very limited space parameter though: a single initial condition with evolution and result very similar to M.C. Vergara et al 2025), to not so promising ones, like computing the Fokker-Planck evolution for the core collapse in a system with relaxation time a factor 1,000 larger that the current age of the Universe (factor 10,000 for the Universe's age at the redshifts of LRDs; F. Panucci et al 2025), being this also in agreement with our statement that $t_{H0} < t_{relax}$ for all LRDs. Our aim instead is to give a more global picture, based on the relevant timescales in the stability of LRDs, in the full variety of properties displayed in their space parameter (for the stellar-only interpretation; Akins et al 2024).

3. Summary and Conclusions

We study the stability and possible fates for LRDs, under the stellar-only interpretation of their observational features. We find that, since LRDs are probably the densest stellar systems ever observed and their cores, the closest to be globally unstable thru runnaway collisions, their nucleus are the most favourable places to find a MBH in the process of formation (or recently formed). We conclude this analyzing three different scenarios in the stellar only interpretation, namely, (i) the numerical prediction of the densest stellar systems simulated so far, (ii) that LRDs real effective radii corresponds to a fraction of the measured upper limits and (iii) that the LRDs core radii corresponds to a fraction of the upper limit sizes, all with the same conclusion: the formation of a VMS by catastrophic runnaway stellar collisions in their nuclear region and subsequently, the possible formation of a MBH from the direct collapse of such VMS.

It is important to note, that we reach to this conclusion thru an analysis of the relevant timescales and the comparison of their observed properties with recent numerical results of the densest stellar systems studied so far (M. C. Vergara et al 2023, 2024, 2025a, b), without the aid any fitting procedure or adjustment of a free parameter. Fitting procedures are restricted to the previously determined parameters of LRDs properties (under the stellar-only interpretation) in Akins et al (2024), their observed redshift range (relevant to give an upper limit for the age of the system; D. D. Kocevski et al. 2024) and the black hole formation efficiency numerically determined in M.C. Vergara et al (2025b) on stellar systems different from LRDs, but not on any part of the analysis in this paper performed for LRDs data.

Since the alternative interpretations for LRDs has either a MBH already existing (R. Maiolino et al. 2024; J. E. Greene et al. 2024) or in the stages of final collapse (L. Zwick et al. 2025; J. Bellovary 2025) and considering that, we showed (under the stellar only

interpretation) that LRDs are the most favourable known places to find a MBH in the process of formation, this unifies the different interpretations for LRDs, into a context of ongoing MBH formation. Therefore, we conclude that under the different interpretations for LRDs, they are candidates to be the most appealing places to host the massive seeds that will later produce the observed population of high redshift quasars, besides the interpretation chosen for their observed properties.

Depending on the discussed interpretations, will be if LRDs are mainly on a runaway stellar collisions stage and early VMS formation, already host a VMS in the stages of final growth and subsequent collapse, or with a MBH just recently formed, depending on their exact place on the described evolutionary stage. The lack of X-ray detections in most of those systems (T. T. Ananna et al. 2024; M. Yue et al. 2024; R. Maiolino et al. 2025), that happens for the MBHs already formed, supports that most LRDs to be in the earlier parts of the mentioned evolutionary path.

The different evolutionary stages predicts different LISA gravitational wave observations (Amaro-Seoane et al. 2013), since a gravitational-wave signal is expected from the final collapsing VMS at the moment of MBH formation, that will be detectable in the LISA band out to high redshift (Sun et al. 2017). Therefore, gravitational wave observations could be discriminator for individual LRDs, among the different evolutionary stages. In addition, the extreme stellar densities needed for this instability could also be happening in merging galactic systems (L. Mayer et al 2010, 2015), like in the almost face-on encounter of the recently discovered infinite galaxy, where it is suggested that a MBH is formed in-situ (P. Van Dokkum et al 2025a). Since the MBHs from the original galaxies are also detected (P. Van Dokkum et al 2025b), this opens the additional possibility for multiple LISA detections from MBHs mergers (J.J. d'Etigny et al. 2024), from a single galactic system.

Finally, a relevant issue not studied at all in this paper is the role of gas in the evolution of LRDs, particularly, in the enhancement of stellar collisions. Although the details of the exact evolution of the gaseous and stellar material are unclear under realistic conditions, results from idealized calculations looks promising (T. Boekholt et al 2018, B. Reinoso et al 2023, 2025) and the dissipative nature of the gaseous component should certainly enhance instabilities. Most likely, the idealized case of extremely dense, purely gas-free LRDs discussed in this paper rarely exists in the early universe, and most often, an unstable LRDs will (partially) collapse during its formation before evaporating its gaseous envelope, as was already proposed in Escala (2021) for (proto-)NSCs at high z. The transitory nature of LRDs in a cosmological context, being a population observed during a cosmic period of only $\sim$1 Gyr in total (i.e. between z $\sim$ 4 and 8; D. D. Kocevski et al. 2024) and also, the extreme stellar densities inferred under the stellar-only interpretation (Guia et al. 2024), makes LRDs the

most appealing places for hosting this (transitory and globally) unstable galactic nuclei.

AE and SV acknowledges partial support from the Center of Excellence in Astrophysics and Associated Technologies (FB210003). L.Z. acknowledges funding through the Alan S. Tetelman 1958 Fellowship for International Research in the Sciences. MCV acknowledges funding through ANID (Doctorado acuerdo bilateral DAAD/62210038) and DAAD (funding program number 57600326). MCV acknowledges the International Max Planck Research School for Astronomy and Cosmic Physics at the University of Heidelberg (IMPRS-HD). DRGS gratefully acknowledges support by the ANID BASAL project FB21003 and thanks for funding via the Alexander von Humboldt - Foundation, Bonn, Germany. ML acknowledges financial support from ANID/DOCTORADO BECAS CHILE 72240058.

REFERENCES

Amaro-Seoane, P., et al. 2013, arXiv:1305.5720

Ananna, T. T., Bogdan, A., Kovacs, O. E., Natarajan, P., & Hickox, R. C. 2024, ApJL, 969, L18

Akins, H. B., Casey, C. M., Lambrides, E., et al. 2024, arXiv e-prints, arXiv:2406.10341

Arca-Sedda M., et al. 2024, MNRAS, 528, 5119A

Askar, A., Davies, M.B., & Church, R.P. 2021, MNRAS, 502, 2682A

Baggen, J. F. W., van Dokkum, P., Brammer, G., et al. 2024, ApJL, 977, L13

Boekholt, T. C. N., et al.2018, MNRAS, 476, 366B

Bellovary, J. 2025, ApJ, 984L, 55B

Binney, J., & Tremaine, S. 2008, Galactic Dynamics, Princeton Univ. Press

Cohn, H. 1980, ApJ, 242, 765C

Dejonghe, H. 1987, MNRAS, 224, 13

Durodola, E., Pacucci, F., & Hickox, R. C. 2025, ApJ, 985, 169

d'Etigny, J., Escala, A. & Rosdhal, J. 2024, ApJ, 971, 38D

Escala, A., 2021, ApJ, 908, 57

Escala, A., 2025, in-prep

Ferrarese, F. , & Merritt, D. 2000, ApJ, 539, L9-L12

Gebhardt, K. et al. 2000, ApJ, 539, L13-L16

Georgiev, I. Y. et al 2016, MNRAS, 457, 2122-2138

Gieles, M., Moeckel N. and Clarke, C.J. 2012, MNRAS, 426, L11

González Prieto, E. et al. 2024, ApJ, 969, 29G

Greene, J. E., Labbe, I., Goulding, A. D., et al. 2024, ApJ, 964, 39

Gultekin, K., et al, 2009, ApJ, 698, 198

Guia, C. A., Pacucci, F., & Kocevski, D. D. 2024, Research Notes of the American Astronomical Society, 8, 207

Harikane, Y., Zhang, Y., Nakajima, K., et al. 2023, ApJ, 959, 39

Henon, M. 1965, AnAp, 28, 62

Inayoshi, K., & Ichikawa, K. 2024, ApJL, 973, L49

Kocevski, D. D., Onoue, M., Inayoshi, K., et al. 2023, ApJL, 954, L4

Kocevski, D. D., Finkelstein, S. L., Barro, G., et al. 2025, ApJ, 986, 126

Loeb, A. 2024, Research Notes of the American Astronomical Society, 8, 182

Madau, P., & Haardt, F. 2024, ApJL, 976, L24

Maiolino, R., Scholtz, J., Curtis-Lake, E., et al. 2024, A&A, 691, A145

Maiolino, R., Risaliti, G., Signorini, M., et al. 2025, MNRAS, 538, 1921

Magorrian, J., et al. 1998, ApJ, 115, 2285-2305.

Matthee, J., Naidu, R. P., Brammer, G., et al. 2024, ApJ, 963, 129

Mayer, L., et al 2010, Nature 466, 1082-1084

Mayer, L., Fiacconi, D., Bonoli, S., et al. 2015, ApJ, 810, 51

Naidu, R., et al. 2025, arXiv e-prints, arxiv:2505.11263

Pacucci, F., Nguyen, B., Carniani, S., Maiolino, R., & Fan, X. 2023, ApJL, 957, L3

Pacucci, F., & Narayan, R. 2024, ApJ, 976, 96

Pacucci, F., Hernquist, L., & Fujii, M. 2025, arXiv e-prints, arXiv:2509.02664

Portegies Zwart, S. F., & McMillan, S. L. W. 2002, ApJ, 576, 899

Rantala, A., & Naab, T. 2025, MNRAS, 542L, 78R

Reinoso, B., et al 2023, MNRAS, 521, 3553R

Reinoso, B., et al 2025, A&A, 700A, 66R

Salviander, S., et al 2008, ApJ, 687, 828

Sun, L. et al. 2017, Phys.Rev.D, 96, 4, 043006

The Event Horizon Telescope Collaboration, 2019, ApJL, 875, L1-L6

van Dokkum, P. et al 2025, ApJ, 988L, 6V

van Dokkum, P. et al 2025, ApJ, 990L, 48V

Vergara, M. C., Escala, A., Schleicher, D. R. G., & Reinoso, B. 2023, MNRAS, 522, 4224

Vergara, M. C., Schleicher, D. R. G., Escala, A., et al. 2024, A&A, 689A, 34V

Vergara, M. C., Askar, A., Kamlah, A. W. H., et al. 2025a, arXiv e-prints, arXiv:2505.07491

Vergara, M. C., Askar, A., Flammini Dotti, F, et al. 2025b, arXiv e-prints, arXiv:250814260

Wang, L., Spurzem, R., Aarseth, S., et al. 2016, MNRAS, 458, 1450

Yue, M., Eilers, A.-C., Ananna, T. T., et al. 2024, ApJL, 974, L26

Zwick, L., Tiede, C., & Mayer, L. 2025, arXiv e-prints, arXiv:2507.22014